Master's Thesis

Title

A Configuration Method of Virtual Networks with Hierarchical Robustness Inspired by the Fractality of Brain Functional Networks

Supervisor

Professor Masayuki Murata

Author

Yoshinobu Shijo

February 12th, 2016

Department of Information Networking

Graduate School of Information Science and Technology

Osaka University

Master's Thesis

A Configuration Method of Virtual Networks with Hierarchical Robustness Inspired by the Fractality of Brain Functional Networks

Yoshinobu Shijo

Abstract

The Internet provides various services which are essential for our daily life as one of the social infrastructure. The number of services provided through the Internet is increasing days by day. However, a long history of developments of Internet causes inflexibility of the today's Internet, that is, it is difficult to integrate modern technology and support new types of requests for services. Recently, the network virtualization attracts a great deal of attention as one of technology to take performance and manageability of services. One of the important research issues for network virtualization is how to embed a request of virtual networks into a physical infrastructure. Another of the important research issues is to investigate what kinds of the virtual network should be constructed dependent on a service request. In this thesis, we focus on the latter issue and investigate a configuration method of virtual networks to provide resilient, efficient, and scalable services to the Internet. Our configuration method is inspired from the fractality of human brain functional networks (BFNs). Fractality is a self-similar property of the topology, and it contributes to robustness and redundant paths in BFNs. Our configuration method piles up a single virtual network as a module in a hierarchical manner and constructs inter-modules links connecting non-hub nodes. Results of numerical evaluations reveal that the fractal topology configured by our proposed method has superior robustness and efficiency. The reachability of the fractal topology is 17% higher than the reachability of non-fractal topology when a 10%-node failure occurs, and the fractal topology relaxes the traffic concentration by about 45% on the most congested node.

Keywords

Fractality

Brain Functional Networks

Hierarchical Robustness

Virtual Network

Hierarchical Modular Network

Contents

List of Figures

List of Tables

1 Introduction

The Internet provides various services which are essential for our daily life as one of the social infrastructure. The number of services provided through the Internet is increasing days by day, such as social media services like movie sharing website and SNS (Social Networking Service), and cloud services including IaaS (Infrastructure as a Service), PaaS (Platform as a Service) and SaaS (Software as a Service). These diverse services are brought by many years of assiduous effort for technology development, not provided from the dawn of the Internet. This long-term development, however, causes inflexibility of the today's Internet, that is, it is difficult to integrate modern technology and support new types of requests for services. For this reason, some network administrators consider to separate network traffic for each service and to use network equipment efficiently and flexibly. Nowadays, network virtualization attracts a great deal of attention as one of technology to take performance and manageability of service. Network virtualization is a technology which enables operating multiple network services independently on a single physical network by separating a physical network and network services. This technology makes the physical network possible to accommodate multiple network services that require different functions or performance [1].

There are many research subjects to develop various technology to implement network virtualization and they have actively been studied in recent years. These researches include, for example, network equipment virtualization such as NIC (Network Interface Card) and router and/or link virtualization such as bandwidth and data-transmit multiplexing, which forms a virtualized network [2]. A virtualized network, or simply virtual network hereafter, is a network which are used by each network service under network virtualization environment.

A virtual network consists of virtual nodes and virtual links. Virtual nodes and virtual links are configured by network administrators, who manage virtual networks, and are embedded in a physical network. For constantly providing network services, it is desired that the connectivity of virtual networks is maintained under failures of physical nodes and links on the physical network including human error of network configurations. Moreover, in the future, larger scale virtual networks may appear by interconnecting existing virtual

7

networks. For example, interconnected and large scale virtual networks correspond to provide advanced and complex network services by combining the basic and simple network services running on a respective single virtual network. According to the report from Ministry of Internal Affairs and Communications in 2015, actually, 46 percent of the performance decay or service stop in telecommunication carrier are caused by the accident in other carrier [3]. To reduce such accidents, it is required to suppress impacts of failures into small range for not affecting the entire network. In addition, there is more traffic flow in the large scale virtual networks. As the scale of topology gets larger, there will be a problem of traffic concentration on a certain node or placements of excess load on network equipment. Virtual networks should be configured as maintaining the connectivity of virtual networks under failures of virtual nodes and links, suppressing impacts of loss of connectivity into small range, and avoiding traffic concentration. In this thesis, we propose a virtual networks configuration methods that achieve robustness in terms of connectivity and relax the traffic concentration.

Our research group focuses on human brain functional networks (BFNs) as clues to configure virtual networks with desired properties. BFNs are networks which show connection structure of brain regions when they perform advanced brain functions. Nowadays, many researchers analyze BFNs as complex network with graph theory [4]. These results reveal the modular structure [5], tradeoff between hop length and wiring cost [6], degree correlation [7] and effects of assortativity [8]. The noteworthy results are that BFNs exhibit fractality [9, 10]. Fractality is one of the topological property that information network topology, such as Internet AS (Autonomous System) level topology, does not exhibit [11]. For this reason, we have studied advantages of fractality of BFNs to network performance from communication network perspective [12]. Our results show the BFN's topology with fractality have many superior paths, or redundant paths, compared to that without fractality. We also show BFNs are robust in terms of connectivity against node failure. Hence, it is expected that virtual networks can possess desired properties by incorporating fractal nature. Note that we explain further details of BFNs in Section 3.

Many previous studies on fractality of network topology analyze only whether the topology has fractality or not. Although some studies propose a generation model of fractal topology, their main objective is eliminating noises which real networks contain

to analyze the pure property of fractal topology. Thus, there are no practical configuration or design methods for the fractal network. In this thesis, we propose a configuration method of virtual networks with fractality. This method configures hierarchical modular virtual networks to integrate fractality, by piling up a single virtual network as a module in a hierarchical manner and constructing inter-modules links via non-hub nodes. Then, we examine the topological performance of fractal virtual networks by comparing to non-fractal networks. Our evaluation results show fractal networks can achieve high reachability and decrease the traffic concentration.

The rest of this thesis is organized as follows. We survey fractality and configuration methods of virtual networks in Section 2. Section 3 explains our results about topological characteristics of brain functional networks. In particular, we show BFNs have fractality in various grain size, and fractality contributes to robustness against node failures and redundant paths in the topology. In Section 4, we propose a configuration method of virtual networks with fractality, and Section 5 shows the performance of the topology configured by our proposed method. We conclude this thesis and refer to future works in Section 6.
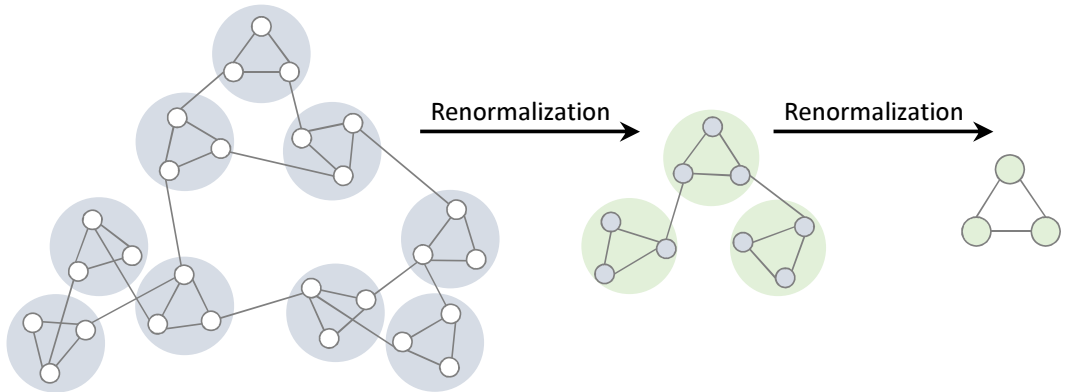
Figure 1: Self-similar property of fractal topology under renormalization

2 Related Work

2.1 What is Fractal?

Originally, a fractal is a geometric concept but is extended for network topology by Song et al [13]. From the point of view of network topology, fractality is a self-similar property or repeating patterns at every scale, as shown in Figure 1. A network topology is fractal when fractal dimension d_b in the topology is a finite value. For calculating d_b, Song et al. proposed a renormalization procedure. This procedure is based on the box-covering algorithm. This algorithm tiles whole nodes in the network topology by "boxes" with size l_B. The size of the box is defined by the maximum hop count between all node pairs in the box. Then, the fractal dimension d_b is calculated by the following relationship,

$$N_B(l_B)/N \sim l_B{}^{d_b}, \tag{1}$$

where $N_B(l_B)$ is the minimum number of boxes and N is the number of nodes in the network topology. When the value of d_b is finite, the relation between box size l_B and number of boxes $N_B(l_B)$ is scale-invariant. In other words, fractality in network topology is the property of preserving the proportion of the number of boxes to the box size. On the other hand, d_B of non-fractal topology is infinite. d_B is appeared as the slope on the log-log graph. Figure 2 shows the relationship among l_B, N_B and d_B on the log-log graph.

Song et al. analyzed fractality of various networks with the renormalization procedure. The analysis showed many networks, such as WWW (World Wide Web), protein interaction networks and cellular networks, have fractality. In their following paper, they

10
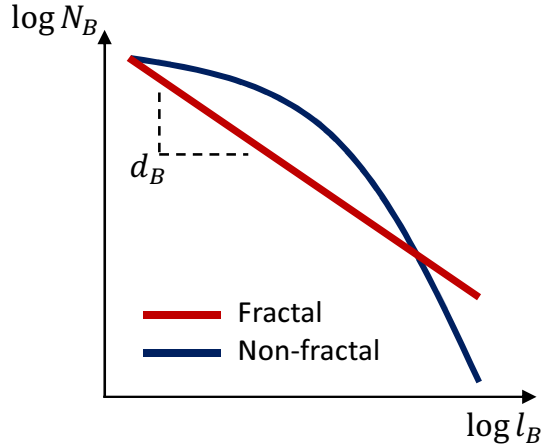
Figure 2: Relationship among box-size l_B, number of boxes N_B and fractal dimension d_B

mentioned that the Internet router-level topology does not possess fractality [11]. The fractal analysis of BFNs is also widely performed, and the results show BFNs have fractality in both anatomical and functional level [10,14]. There are several works of re-analyzing the networks which were well studied in the past with fractal theory [15]. The analysis of the performance of the fractal network, however, have not been carried out. Therefore, advantages of fractality to communication networks have been still unknown.

2.2 Generation Model and Essentials of Fractal Topology

Some generation models of fractal topology are proposed in previous studies [11, 16, 17]. Here we explain the model by Song et al. The model is simple but useful to understand the essentials or origins of fractality.

The model is based on the inverse of the renormalization procedure. In this model, the network grows as the time step t increases. Every node at step $t-1$ with degree $k(t-1)$ evolves to a box and $mk(t-1)$ additional nodes are generated inside each box at step t. Nodes existing at step $t-1$ are connected to all the generated nodes inside each box. In addition, all links at step $t-1$ are removed and new cross-box links are generated between nodes inside each box. They proposed two kinds of mode to generate cross-box links, that is, Mode I and Mode II. In Mode I, two boxes are connected through a direct link between their hubs. In Mode II, a cross-box link connects to their non-hubs or additional nodes at step t. The network evolves through the combination of Mode I with probability e and

Mode II with probability $1 - e$, where e is defined as the measurement of the level of hub attraction.

The probability e decides the fractality of topology generated by the model. The topology with higher probability e, or hub attraction, tend to be non-fractal, on the other hand, the topology with lower probability e, or hub repulsion, are inclined to be fractal. This behavior is the essentials of fractal topology, that is, hub repulsion is the cause of fractality.

2.3 Relation between Hierarchical Modularity and Fractal

A module is a group of nodes which are densely connected each other inside the module and sparsely connected to nodes outside the module. A hierarchical module is a group of modules connected in a hierarchical manner. A topology has hierarchical modularity if the topology has fractality. Gallos et al. [14] explains this relationship through the property of resulting boxes obtained by the box-covering algorithm. The box-covering algorithm detects boxes that contain a maximum number of nodes within each box at given length scale l_B. As a result, the boxes tend to maximize modularity. Different values of the length scale l_B produce boxes of different size. These boxes are identified as modules at various length scale, then, modules at a smaller scale l_B are merged into larger entities as increasing l_B. Thus, a fractal topology has hierarchical modular structure. Considering the contrapositions, topology without hierarchical modularity cannot have fractality.

Meanwhile, a hierarchical modular topology does not always have fractality. It is evident from the Song's generation model with higher probability e.

2.4 Configuration Methods of Virtual Networks

There are few studies on configuration methods of virtual networks. VNE (Virtual Network Embedding) problem is the major problem treating virtual networks. In this research problem, researchers randomly configure virtual network topology just for evaluations, therefore, they do not focus on the virtual network itself. A few study has focused on constructing virtual networks [18] In [18], Guo et al. studied survivability against facility node failures. They proposed a method to efficiently re-embed virtual nodes in a physical

network for sustaining availability of virtual networks when facility failures occur. They, however, do not refer to the configuration method of virtual networks which can sustain connectivity against node failure.

3 Fractality and Performance of Brain Functional Networks

3.1 Fractality Analysis

3.1.1 Topology Data

Generally, brain functional network topology is obtained by processing data from the fMRI measurement. By using fMRI, we can obtain time-series data of brain activities at each voxel. A voxel is a unit of fMRI measurement. It can be regarded that there are brain-functional interactions between voxels which showed high-correlated brain activity transition. Thus, by regarding a voxel as a node and by constructing a link between voxels where correlation value for brain activity transition is more than given threshold, we can obtain the brain functional network topology that reflects brain-functional interactions [4]. Note that the obtained topology may be disconnected depending on the threshold. In this case, the only most giant connected component is generally used for analysis.

We obtained the brain functional network topology for analysis by using the method explained above. There is one male subject under resting-state conditions, and we measured subject's brain activities with fMRI. The data from fMRI often include measurement errors. To remove errors, we applied motion correction, or realignment, and slice timing correction by using SPM8 [19]. Then we calculated a correlation value between all voxels by Pearson's method. Taking into account topology scale, we set the threshold to 0.65 and obtained the topology with 10823 nodes and 64275 links. Hereafter, we call this topology as voxel-level topology.

3.1.2 Decomposition of Voxel-level Topology

The voxel-level topology has almost no relevance to brain functions because a voxel is merely a measuring point of fMRI and it does not directly relate to brain functions. It is needless to say that it is important to focus on brain functions about our analysis of BFNs. So we should obtain brain-functional-level topology. There are some methods to obtain that kind of topology, such as ROI (Region Of Interest) which provides brain functions by anatomical position of voxels. We, however, want to focus on fractality and hierarchical module structure brought by it. Therefore, we obtain module-level topology as brain-

functional-level topology by regarding module as a node at various grain scales. A module is an aggregation of high-correlated nodes at voxel-level topology, so we can regard modules as brain functions. Various grain scales of voxel-level topology correspond to levels of brain functions, where small scale corresponds to primitive functions and large scale corresponds to derivative functions. Note that we can decompose the topological structure of voxel-level topology into 3 types of topological structures; module-level topology, inner-module topologies, and inter-module links. We explain how to obtain these structure.

For obtaining module-level topology at various grain scales, we first detect hierarchical modular structure. We use so-called "Louvain method [20]" for this purpose. This method can find module identifier $M_i(h)$ of node i at PATH (hierarchy) h[1]. We obtained module-level topology at PATH h by following procedures:

Step.1 Generate initial topology. The number of nodes is set to the number of modules at PATH h. The number of links is set to zero.

Step.2 Construct a link between nodes $M_i(h)$ and $M_j(h)$ when a link exists between node i and node j at voxel-level topology and satisfies $M_i(h) \neq M_j(h)$.

Note that we call voxel-level topology as module-level topology at PATH 0 for convenience. Table 1 shows the number of nodes and links of the obtained module-level topology.

Inner-module topology at PATH h consists of voxel-level nodes with same module identifier at PATH h. That is, the inner-module topology can be obtained as a subgraph of the voxel-level topology. For each PATH-level, the voxel-level topology can be decomposed into a set of inner-module topologies. We distinguish inner-module topologies by the rank of module size in descending order of the size.

Inter-module links are links connecting different modules. That is, they are set of links obtained by removing all links of inner-module topologies from voxel-level topology.

As an example, Figure 3 is the illustration of the decomposition of voxel-level topology with 26 nodes. A group of nodes surrounded by a circle is a module. The nodes in the same module have same module identifier. This voxel-level topology contains six modules at PATH1, three modules at PATH2, and one module at PATH3. Module-level topology at PATH1 and PATH2 obtained by applying procedures explained above is illustrated

---

[1]We call the level of hierarchy as "Path" by following [20].
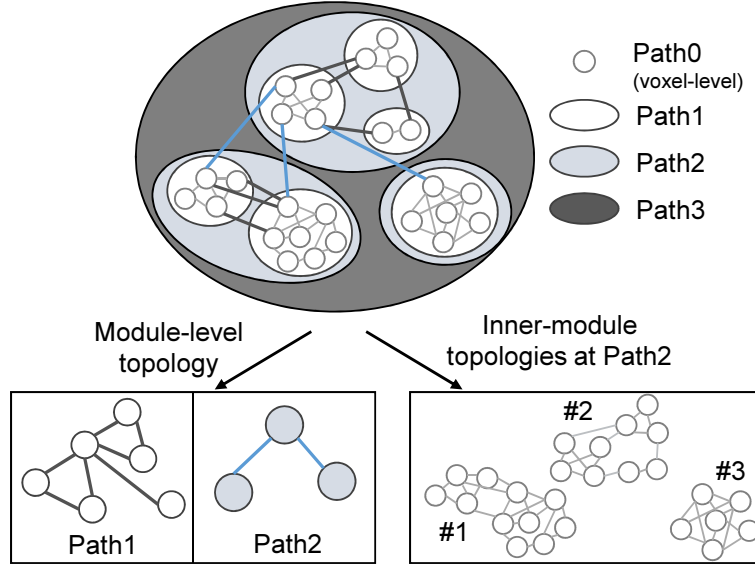
Figure 3: Illustration of decomposition of BFN's voxel-level topology

Table 1: The number of nodes and links at each PATH by decomposition of BFNs

PATH	# of nodes	# of links
0	10823	64275
1	1116	1946
2	203	458
3	79	245
4	69	222

at the left bottom of the Figure 3. Even if there are multiples links between modules at voxel-level topology, they are regarded as a single link at the module-level topology. Thus, we can obtain module-level topology with six nodes and seven links at PATH1 and with three nodes and two links at PATH2. On the other hand, inner-module topologies at PATH2 is illustrated at the right bottom of the Figure 3. We can obtain three inner-module topologies at PATH2 because there are three modules at PATH2. The number of nodes of each inner-module topology is eleven, nine, and six from the left. Therefore, the rank of module size is assigned one, two, and three from the left.

(a) Voxel-level and module-level topology　　　(b) Inner-module topology (PATH1)
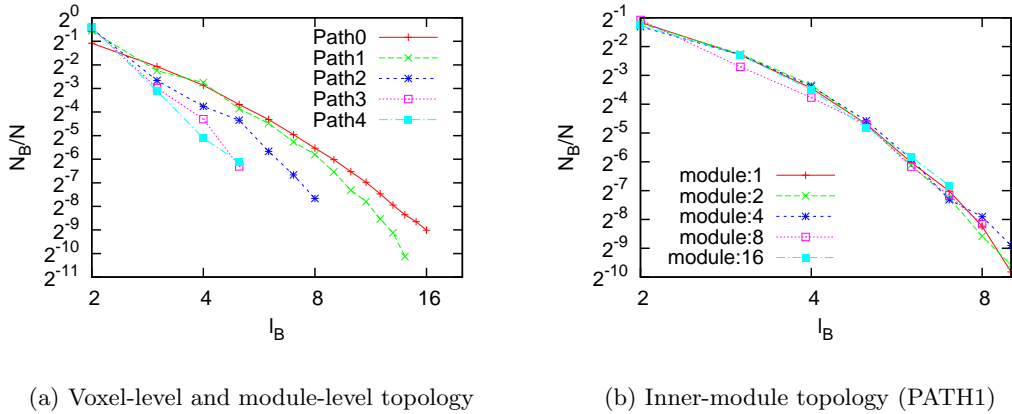
Figure 4: Fractality of BFN

3.1.3　Results

We analyzed fractality of both module-level topology and inner-module topologies. The results are shown in Figure 4. Although there are about 1500 or more inner-module topologies over four PATHs, inner-module topologies with a sufficient number of nodes, more than 100 nodes, share the similar result. Then, as the result of inner-module topologies, we show only the topologies at PATH1 with module number 1, 2, 4, 8 and 16. The figure shows N_B decays against l_B at the power-law manner in all topologies, therefore, they are fractal topologies.

3.2　Path Quality Evaluation

3.2.1　Methods

For evaluating path quality, it is to be desired that we derive all paths between any nodes, calculate the hop count along the paths and compare the distribution of the hop count with other comparison topologies. It is, however, almost impossible due to very long computation time. Then, taking computation time into account, we derive from shortest path to 300th path between any nodes in the topology, and calculate the hop count. We use Yen's K shortest paths algorithm [21] for calculating paths. Defining H_K as the average hop count of K-the shortest path between arbitrary node pair, we take a distribution from H_1 to H_{300} as metrics for path quality.

17

3.2.2 Topologies for Evaluation

In this paper, we evaluate BFNs' path quality by comparing with various topologies. We examined following topologies obtained by network generation models for comparison. These models are used in the field of neuroscience and/or reflect a part of structural properties of BFNs.

- Random model

- Barabási-Albert (BA) model [22] which reflects the structural property of power-law degree distribution.

- Watts-Strogatz (WS) model [23] which reflects the integration of local optimality and global efficiency [24].

- Waxman model [25] which reflects the property that functional modules in anatomically close position are densely connected [26].

We evaluate the module-level topology from PATH1 to PATH4 respectively. The topologies for comparison are generated with models so that the number of nodes and links of those corresponds to module-level topology at each PATHs. Note that WS and Waxman model have several parameters. WS model has parameter p which is the proportion of random swapping of links. We calculated the average hop count $H(p)$ and clustering coefficient $C(p)$ against p, and obtained the results. Figure 5 shows the result at PATH1 and almost same results as PATH1 are obtained at other paths. Regarding high clustering coefficient as local optimality and the low average hop count as global efficiency, the value of p should be around 0.1 to integrate high clustering coefficient and the low average hop count. Therefore, we assign parameter p to 0.1 for WS model. On the other hand, Waxman model has parameters α and β. They influence the probability to have a link between node u and node v defined by

$$P(u,v) = \alpha e^{-d(u,v)/\beta L}, \tag{2}$$

where $d(u,v)$ is the distance between u and v, and L is the maximum distance between any two nodes. The value of α affects the number of links in the topology. When the
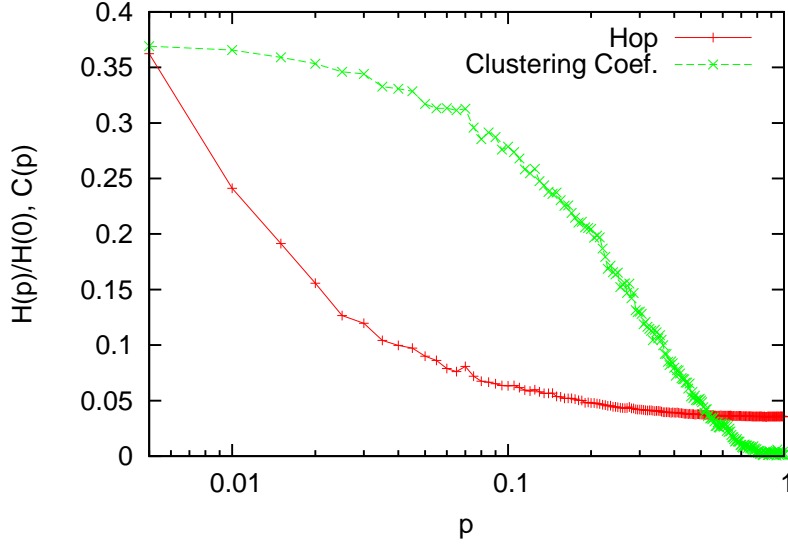
Figure 5: The value of the average hop count $H(p)$ and clustering coefficient $C(p)$ with the proportion p of random link swapping in Watts-Strogatzs model

value of α is higher, the generated topology has more links. However, the number of links of the comparison topology corresponds to that of module-level topology in this paper. Hence, we assign α to 1.0 and modify WS model to generate topology with given number of links. The value of β affects the probability of having a link between nodes with a certain distance. When the value of β is lower, the fewer links are constructed between nodes with long distance, or nodes with short distance have more links. Therefore, we assign β to 0.1 for reflecting property that nodes in close position are densely connected.

3.2.3 Results

Figure 6 shows distribution from H_1 to H_{300} of topologies for evaluation. Focusing on BFNs, or red line, the value H_K is minimum for overall K at PATH1 and PATH2. At PATH3 and PATH4, H_K is minimum for almost overall K. Even in the case that H_K is not minimum, H_K is small enough comparing with other topologies. Therefore, it can be concluded that BFNs have many superior paths at the module-level topology.

(a) PATH1 (b) PATH2

(c) PATH3 (d) PATH4
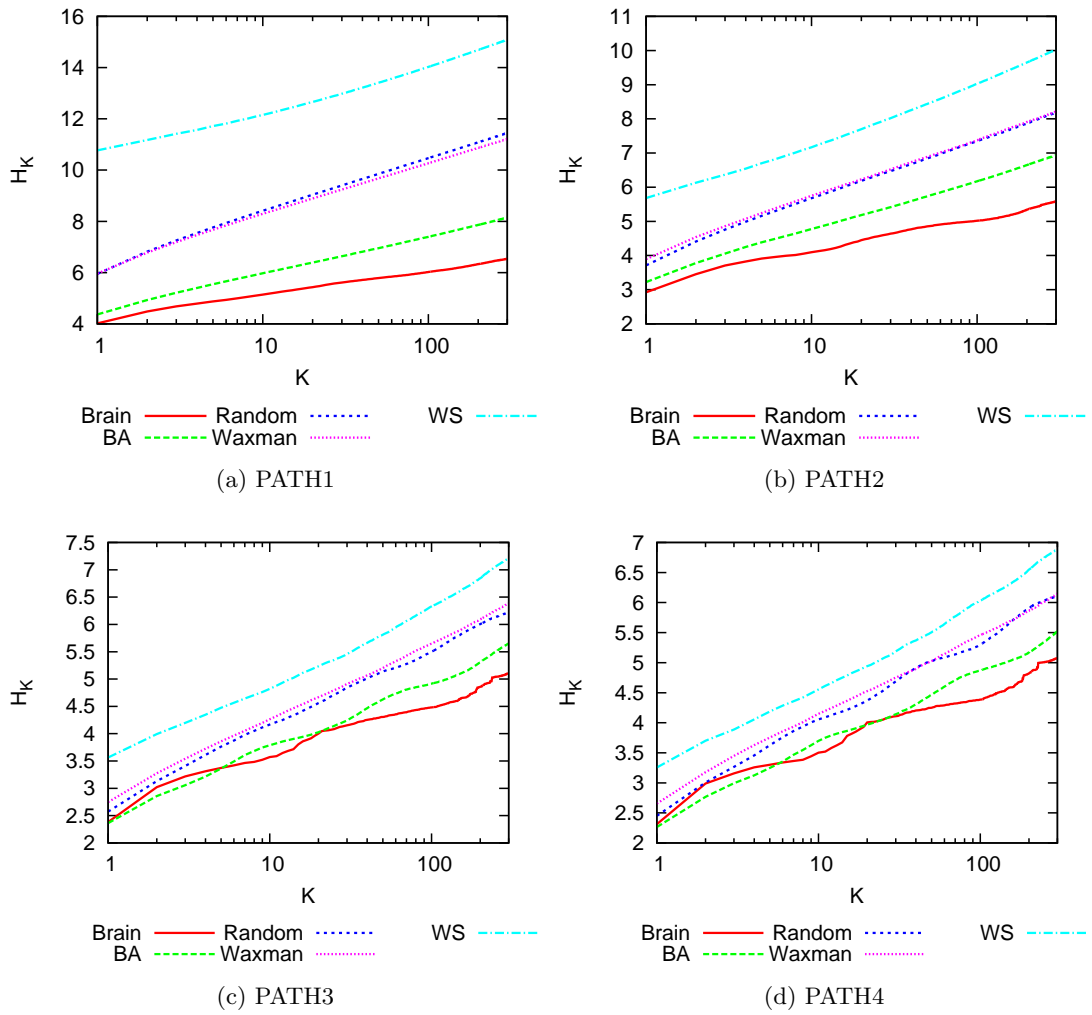
Figure 6: Distribution of average hop length from 1st to 300th shortest paths of the topologies for evaluation

20

3.3 Robustness Evaluation

3.3.1 Methods

In Ref. [11], the authors evaluate the robustness of fractal and non-fractal topologies. They use the relative size of the largest cluster, S, and the average size of the remaining isolated clusters, $\langle s \rangle$ as a function of the removal fraction f of the largest hubs of topologies for evaluation. In this paper, we follow its evaluation method. This method, however, can evaluate only single topology, or cannot evaluate robustness relationship between topologies at the different hierarchy. We want to evaluate such relationship to focus on hierarchical module structure brought by fractality. Therefore, we generate module-level topology under the removal fraction f_0 of the nodes at PATH0 and calculate S and $\langle s \rangle$ of each module-level topology. For failure scenario, Ref. [11] considers only hub node failure, that is, a node with the highest degree in the topology is removed one by one until removal fraction f reaches a certain threshold. We, in addition, consider random node failure, that is, a randomly chosen node is removed. We set removal fraction threshold to 0.50 by the Ref. [27].

3.3.2 Topologies for Evaluation

We focus on fractality of BFNs, so we evaluate the influence of fractality on robustness. Here we evaluate two types of topology, fractal and non-fractal voxel-level topology, preserving the topological structure at module-level.

Fractal topology is brain functional network topology, so we use it for evaluation. On the other hand, non-fractal topology should be generated by some method. The easiest way is to use topology generation model for non-fractal topology. Topology obtained by this model, however, cannot preserve the module-level topological structure of BFNs. Here we apply the essence of non-fractal generation model to generate the desired topology, as we mentioned in Section 2.2. We rewire inter-module links of BFNs so that hub node in each module construct inter-module links. Thus, we obtain non-fractal voxel-level topology with preserving the topological structure at module-level.

Now we confirm the fractality. Figure 7 shows distribution of l_B versus N_B for brain functional network topology and corresponding non-fractal topology. The result reveals
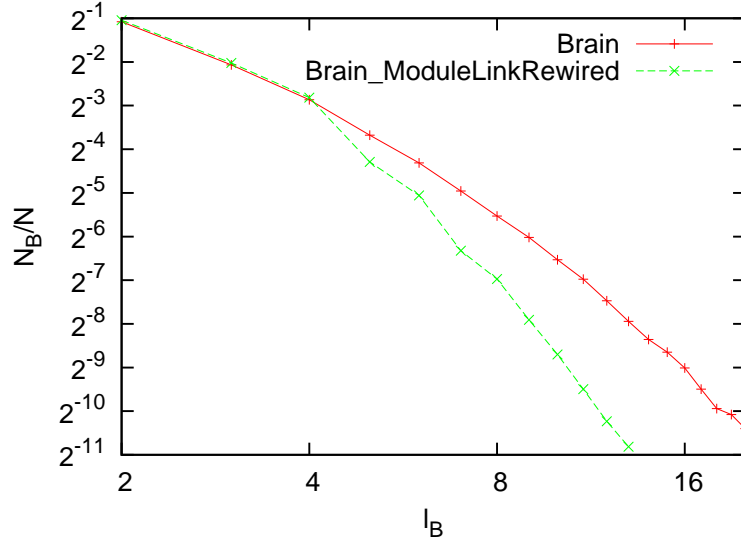
Figure 7: l_B versus N_B distribution of brain functional network topology and non-fractal topology

that fractality is changed so that fractality of the rewired topology is weakened.

3.3.3 Results

We show evaluation results of hub node and random node failure respectively in following paragraphs.

Hub node failure Figure 8 shows the result of hub node failure and shows a similar tendency for all the case of PATHs. Focusing on S, although both network topologies break down as removal fraction f_0 increases, brain functional network topology is the significantly slow pace of breaking down. This means brain functional network topology has the significantly higher robustness to hub node failure at both of voxel-level and module-level topology.

Here, focusing on same f_0 for brain functional network topology, the value S is larger at higher PATH. This means module-level topology at higher PATH is more robust than topology at lower PATH.

Random node failure   We generate 50 patterns of a random node failure and calculate S and $\langle s \rangle$ for each pattern. Then we derive worst and average results from all pattern results. Note that the worst result is based on S at each PATH independently, that is, we select minimum S from 50 patterns at a certain f_0.

Figure 9 shows the worst result. In the same way, hub node failure, brain functional network topology has the significantly higher robustness to worst-case random node failure. Figure 10 shows the average result. Both topologies share almost same transition of S and $\langle s \rangle$ as f_0 increases. This means that both topologies have the almost same robustness to average-case random node failure.

Taken together with hub node failure, brain functional network topology is more robust than corresponding non-fractal topology.
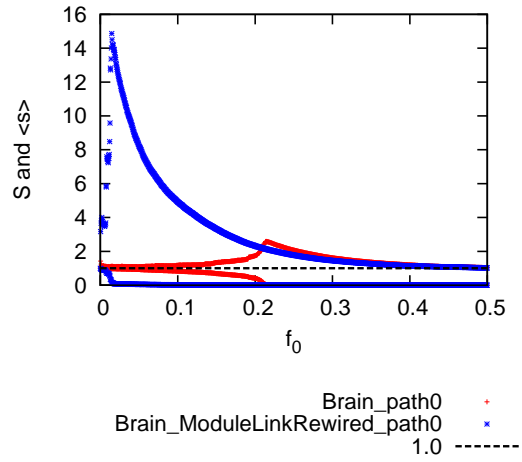
(a) PATH0
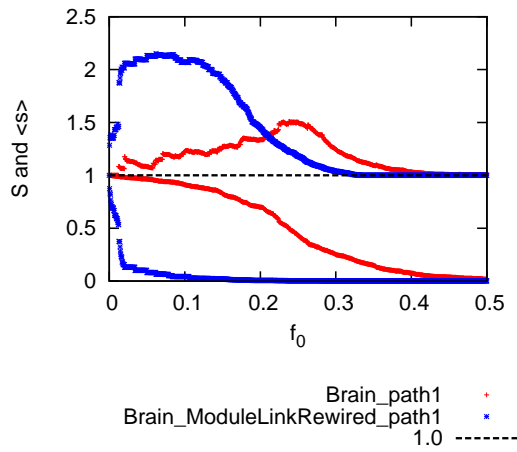
(b) PATH1
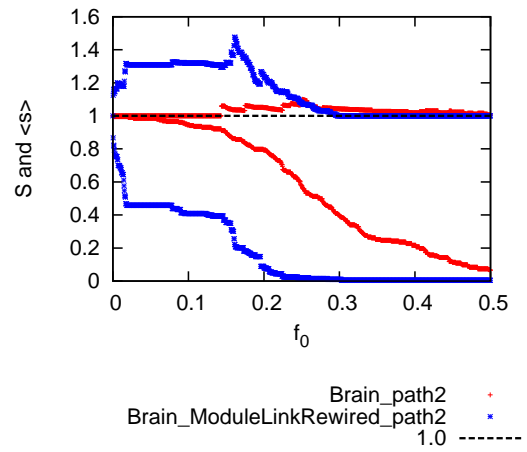
(c) PATH2
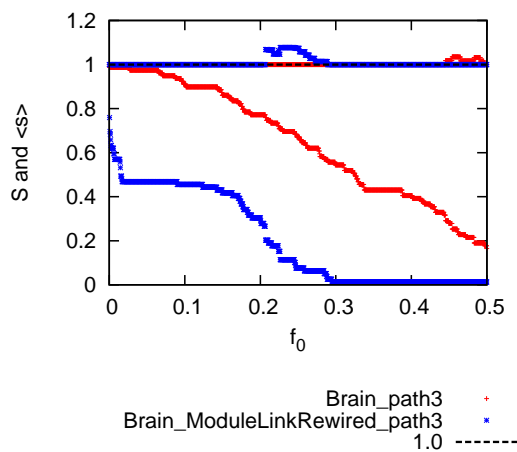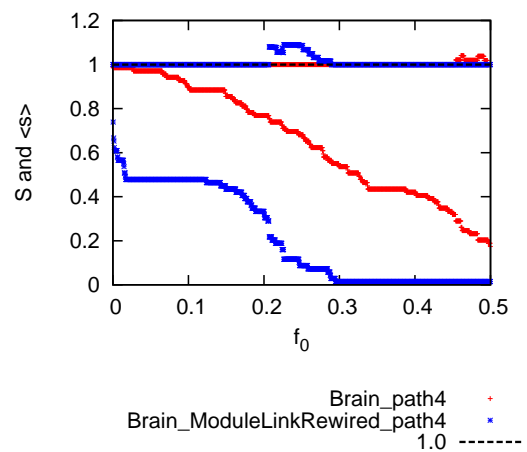
(d) PATH3

(e) PATH4

Figure 8: Cluster size transition under hub node failure
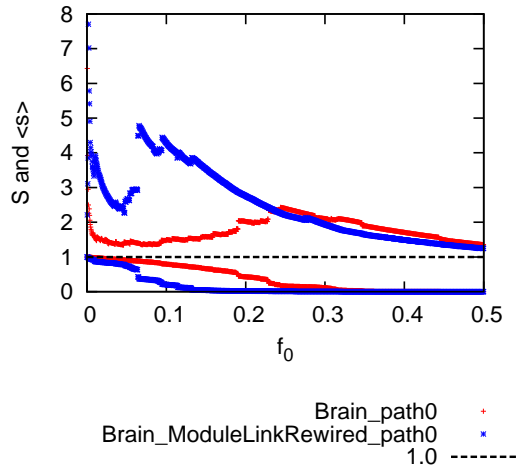
(a) PATH0
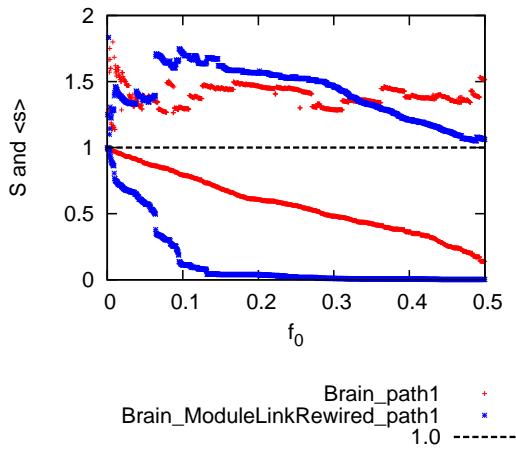
(b) PATH1
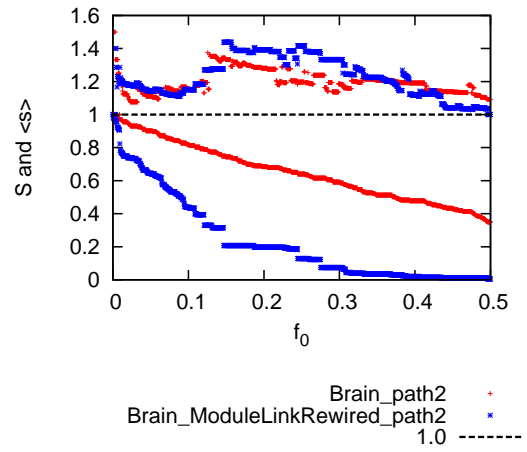
(c) PATH2
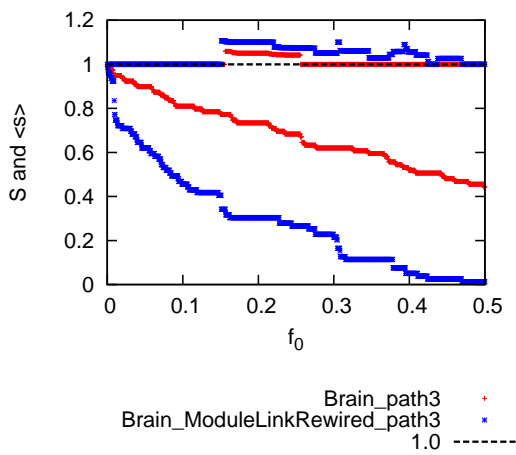
(d) PATH3
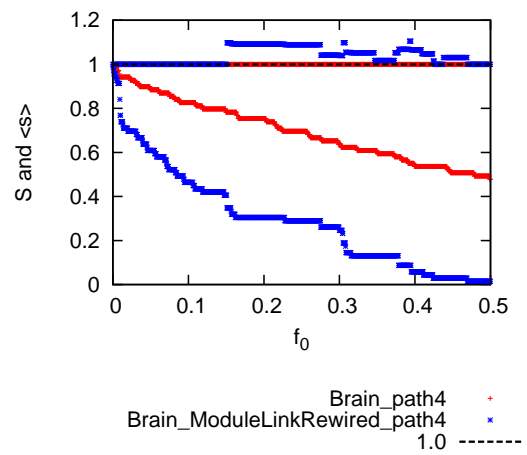
(e) PATH4

Figure 9: Worst case of cluster size transition under random node failure

(a) PATH0

(b) PATH1

(c) PATH2

(d) PATH3

(e) PATH4
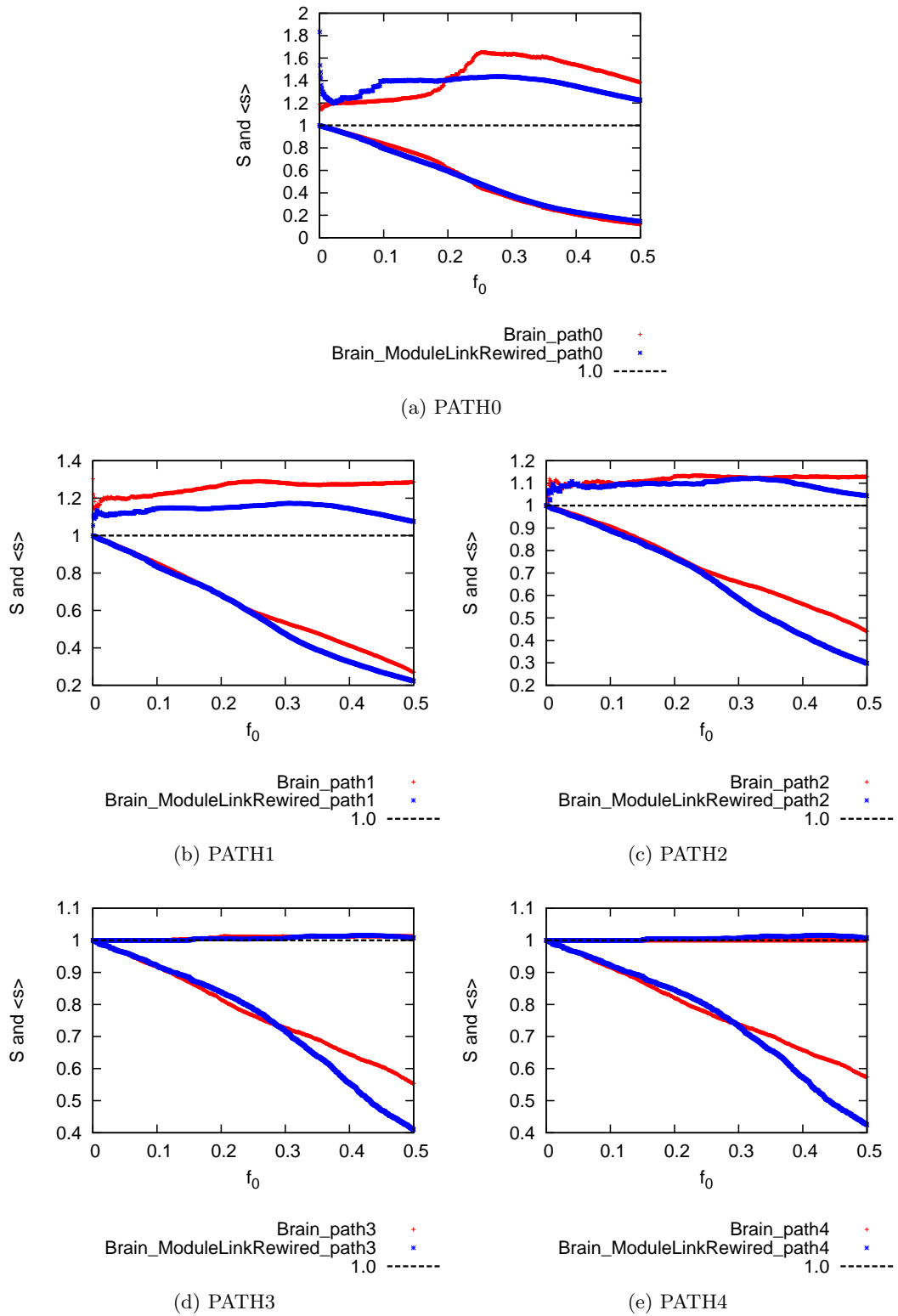
Figure 10: Average case of cluster size transition under random node failure

4 Hierarchical Modular Virtual Networks with Fractality

4.1 Virtual Networks as Hierarchical Modular Networks

As we mentioned in Section 2.3, the topology with fractality needs to have hierarchical modular structure. Here we assume that virtual networks which we configure in this thesis have a hierarchical modular structure for fractality.

To attain hierarchical modular structure, we regard a single virtual network as a module, and we aim to configure a whole virtual network by hierarchically interconnecting single virtual networks. A single virtual network provides small and basic services from the perspective of whole virtual networks, and we regard that it is configured by its administrators. In other words, we exclude a single virtual network from the configuration of our method.

4.2 Construction of Hierarchical Structure

We implement hierarchical modular structure by using BHMN (Basic Hierarchical Modular Network) model proposed in Ref. [28]. As shown in Figure 11, this model regard a topology at hierarchy $h - 1$ as a module, and the topology at hierarchy h is generated by interconnecting these modules. The method for generating topology at each hierarchy is as follows:

Hierarchy 1 (lowest) Any topology with LN nodes and LL links. The link density, or ratio of the number of links against the total number of combinations of nodes, is ρ_1.

Hierarchy $h(\geq 2)$ Connecting two topologies at hierarchy $h - 1$ as modules. The link density between modules is ρ_h.

The link density ρ_h is calculated by the following equation:

$$\frac{\rho_2}{\rho_1} = \frac{\rho_3}{\rho_2} = ... = \frac{\rho_h}{\rho_{h-1}} = d \in (0, 1). \tag{3}$$

Equation (3) means the topology at upper hierarchy has less inter-module links. Lower d can generate a topology with clear hierarchical structure.
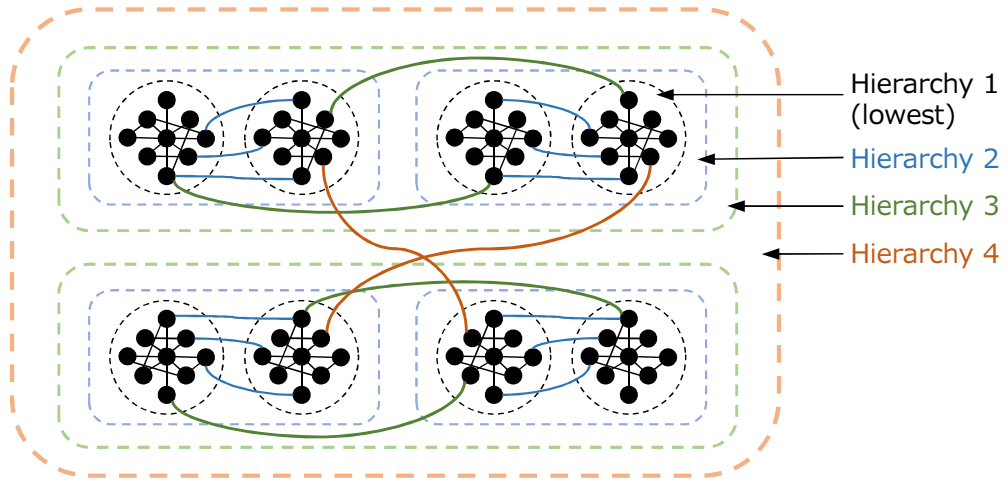
Figure 11: A topology with BHMN model for explanation : $m = 2$

BHMN model configures a topology at hierarchy h by connecting two topologies, or modules, at hierarchy $h - 1$. Here we introduce parameter m to change the number of modules. When generated topology has the same number of nodes, lower m generates a "narrow and high" topology, on the other hand, higher m generates a "fat and low" topology. When parameter m is greater than three, we should consider the topology at module-level. Here we use star topology as module-level topology.

4.3 Strategies for Connecting Modular Networks for Changing Fractality

As we refer in Section 2.2, fractality is affected by degree correlation, especially the connection structure of hub nodes. In the case of not configuring the topology at lowest hierarchy in BHMN model, degree correlation of topology is decided only by the connection structure of inter-module links. In other words, the topology with various fractality can be generated by changing the method of construction of inter-module links. We use two types of methods for constructing inter-module links.

The first method is to construct links between nodes which are independently selected from each module by the following equation:

$$P(d_i) = \frac{(d_i)^\alpha}{\Sigma_j (d_j)^\alpha} \tag{4}$$

It is confirmed that various degree correlation can be achieved by changing the parameter
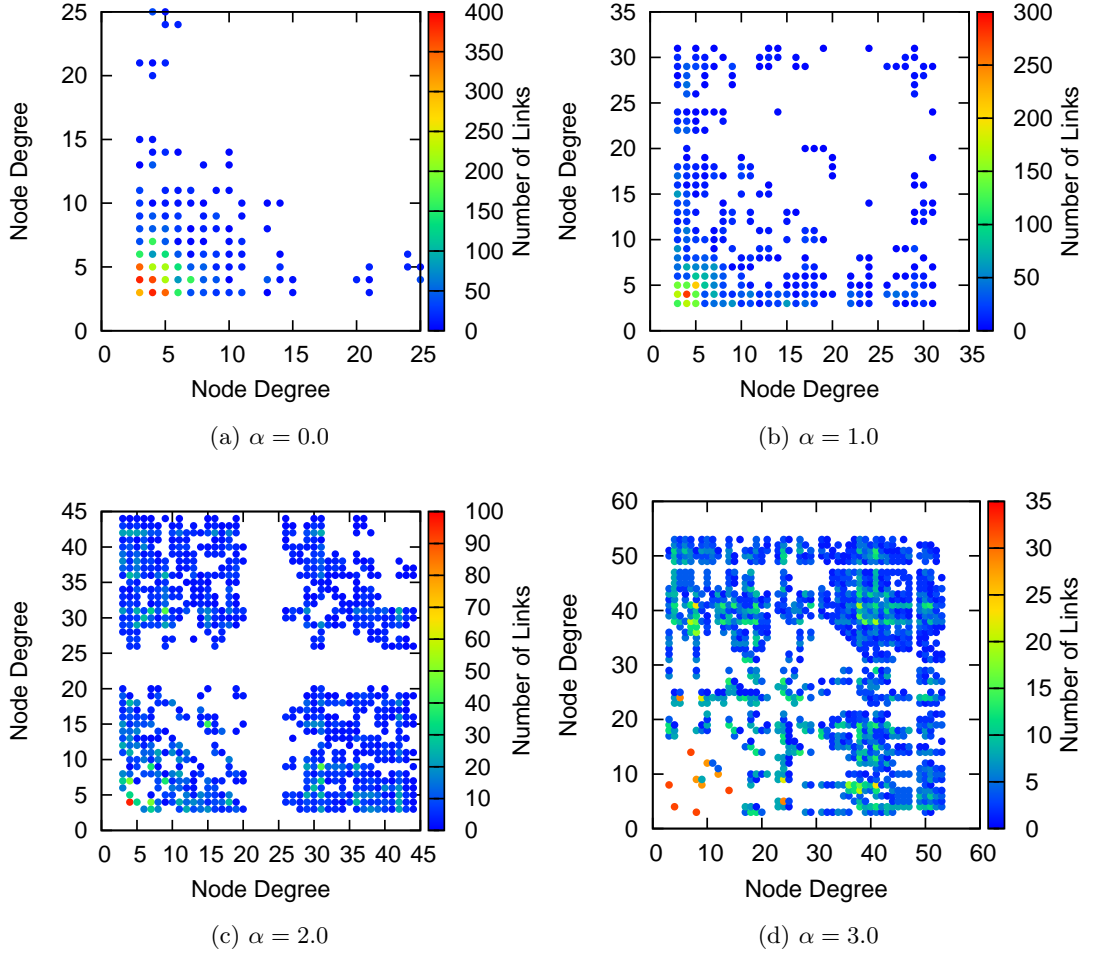
Figure 12: Relations between parameter α and degree correlation of inter-module links

α in Equation (4). As one of examples, Figure 12 shows degree correlation of inter-module links when α is set to 0.0, 1.0, 2.0 and 3.0. Both x-axis and y-axis are node degree of both sides of inter-module links, and colors of plot represent the number of inter-module links between corresponding node degree. It is obvious that, when α is small, there are many links between non-hub nodes and a few links between non-hub and hub nodes. As α increases, while the number of links between non-hub nodes decreases, more links between hub nodes are constructed.

The second method is to minimize the metric $S_M(G)$. $S_M(G)$ derives from considering only inter-module links in the metric $S(G)$. $S(G)$ is the metric which can identify the connection structure of hub nodes and larger value means the dense connection of hub

nodes [29]. $S_M(G)$ is defined as following equation:

$$S_M(G) = \sum_{(i,j) \in E_M} d_i d_j, \tag{5}$$

where, in two graphs $G_1 = (V_1, E_1)$ and $G_2 = (V_2, E_2)$, $E_M \subset V_1 \times V_2$ is set of inter-module links, and d_i denotes the degree of node $i \in V$. As Equation (5) shows, minimizing $S_M(G)$ means that inter-module links are constructed between small degree nodes as much as possible. Note that maximizing $S_M(G)$ is the one of the methods of constructing inter-modules links. We, however, do not consider this one. This is because, when $S_M(G)$ is maximized, inter-module links are concentrated at certain nodes, and the generated topology is significantly vulnerable to failure of these nodes. This is clearly not the topology we aim to configure.

4.4 Fractality Validation

Here, we validate that our proposed method can configure the topology with and without fractality depending on strategies for the construction of inter-module links and the parameters.

4.4.1 Parameter Settings

Our configuration method has roughly five parameters. For the validation of fractality, we set parameters as shown in Table 2. Parameters m and h affect the number of nodes of the generated topology. We assign (m, h) to $(2, 7)$, $(4, 4)$, $(8, 3)$, $(64, 2)$ to generate the topology with 8192 nodes. Note that the topology at lowest hierarchy is generated by BA model.

The number of inter-module links should be decided by parameter d, however, we do not apply it in the case of $m \geq 3$. This is because the generated topology has the same number of nodes but a different number of links. For example, the number of links with $d = 0.20$ is 14261 for $m = 2$ and 21188 for $m = 4$. Here, as a reference, we use the number of links in the topology with $d = 0.20$ and $m = 2$. For generating the topology with the same number of links, we use a constant number of inter-module links at each hierarchy for a topology with $m \geq 3$, as shown in Table 3. Then all topology have 14261 links.

Table 2: Parameters of our proposed model

Parameter	value	description
LN	128	the number of nodes at lowest hierarchy ($h = 1$)
LL	256	the number of links at lowest hierarchy ($h = 1$)
d	0.20	the proportion of ρ_h to ρ_{h-1} (use only at $m = 2$)
m	2, 4, 8, 64	the number of topologies at hierarchy $h-1$ to construct topology at hierarchy h
h	depends on m	the number of hierarchy of generated topology

Table 3: The number of inter-module links in our proposed model with different parameters (m, h)

		(m, h)		
		$(4, 4)$	$(8, 3)$	$(64, 2)$
	2	36	34	32.3
Hierarchical level	3	22	19	
	4	15		

We consider following five patterns to construct inter-module links. Note that we use C[α'] as the notation in the case of $\alpha = \alpha'$ in Equation (4).

- MINSG: $S_M(G)$, defined as Equation (5), is minimized

- C[$\{0.0, 1.0, 2.0, 3.0\}$]: parameter α in Equation (4) is assigned as 0.0, 1.0, 2.0 and 3.0

4.4.2 Results

The results are shown in Figure 13. The figure shows that, for C[1.0], C[2.0] and C[3.0] regardless of the parameter m, N_B decays exponentially against l_B, therefore they are non-fractal topology. On the other hand, the topologies generated by MINSG and C[0.0] have fractality when parameter m is 2, 4 or 8. In the case of $m = 64$, no topologies have fractality. This is because there is no hierarchical structure as $h = 2$ when $m = 64$. A

31

(a) m=2

(b) m=4

(c) m=8

(d) m=64
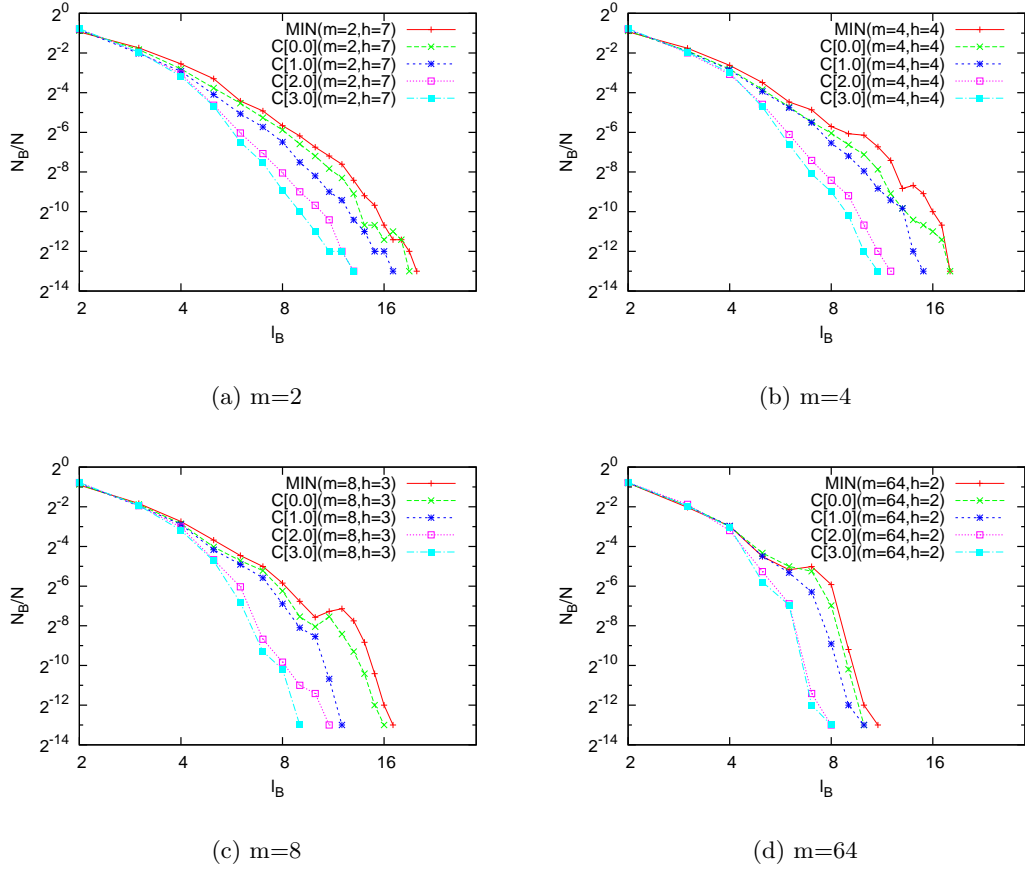
Figure 13: Fractality validation of our proposed model : $N = 8192$

fractal topology needs hierarchical structure, hence the topology with $m = 64$ cannot have fractality.

To summarize, the topology has fractality when parameter m is 2, 4 or 8, and inter-module links are constructed by the methods of MINSG or C[0.0]. In contrast, the others do not have fractality. These results mean fractality of the topology can be controlled by changing the strategies for construction of inter-module links in BHMN model.

5 Performance Evaluation

In this section, we evaluate the performance of fractal topology compared to non-fractal topology. Our objectives to configure fractal topology are to maintain the connectivity, suppress impacts of loss of connectivity into a small range and avoid traffic or load concentration. Therefore, as performance metrics, we use reachability between modules under node failure and node betweenness centrality. In addition, we consider average hop length and diameter to assess the fundamental performance of topology. Their evaluation results are shown in following subsections.

5.1 Topologies for Evaluation

Here we aim to reveal the relationship between fractality and topological performance. In Section 4.4, we clarified which topology has fractality or not. Therefore, we use same topologies in Section 4.4 for evaluation in this section. In other words, the parameters are set as shown in Table 2 and they generate topology with 8192 nodes and 14261 links.

In addition, for the evaluation of node betweenness centrality and hop length, we evaluate large-scale topology to evaluate the influence of topology growth. For that, as parameters (m, h) are assigned to $(2, 8)$ and $(2, 9)$, we generate the topologies with 16384 and 32768 nodes.

5.2 Reachability under Node Failure for Robustness Evaluation

5.2.1 Metrics

As we mentioned in Section 1, it is important to maintain the connectivity of virtual networks under failures, and it is desirable to suppress impacts of failures into small range for not affecting entire network even if the connectivity losses. For evaluating this property, we introduce the metrics defined as follows:

$$T_f^h = \frac{\left|\{(M_x^h, M_y^h) \mid \text{exists paths between } (x, y) \in V^1,\ M_x^h \neq M_y^h\}\right|}{|N^h| \times |N^h - 1|} \in [0, 1], \qquad (6)$$

where V^1 is the set of nodes in topology at lowest hierarchy, M_x^h is the module number of node $x \in V^1$ at hierarchy h, and N^h is the number of modules at hierarchy h. Note
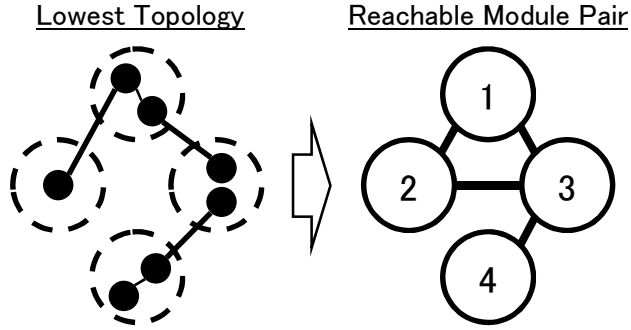
Figure 14: The robustness metrics T_f^h

that T_f^1 can be defined by regarding each node at lowest hierarchy as a module, that is, $\forall x \in V^1 (M_x^1 = x))$.

Now we explain the metrics by using Figure 14 as a concrete example. The left side of this figure shows two levels of the topology at failure ratio $f = f_x$; the node at lowest hierarchy as a black-colored circle, and the module at hierarchy $h = h_y$ as a dotted circle. The right side of this figure shows reachable modules at hierarchy h_y based on the topology on the left side of this figure. Then the values of the numerator and denominator of $T_{f_x}^{h_y}$ are as follows:

$$(numerator) = |(1,2),(1,3),(2,3),(3,4),(2,1),(3,1),(3,2),(4,3)| = 8,$$

$$(denominator) = 4 \times (4-1) = 12,$$

and $T_{f_x}^{h_y}$ is calculated as $= 8/12 = 0.75$. This means that one-fourth of module pairs at hierarchy h_y no longer can communicate each other.

5.2.2 Failure Scenario

We consider three failure scenarios. The first one is the failure of both terminal nodes of inter-module links. This failure simulates the case that nodes exceed its capacity due to a large amount of traffic exchange between modules. We randomly select inter-module links and remove the nodes connected to inter-module links. This procedure is repeated until all inter-module links are removed from the topology. The second one is the random node failure. In this scenario, the randomly chosen node fails. This corresponds to various types of natural failures such as human errors, natural disasters, and so on. The last one is the

hub node failure. The node with the largest degree fails in this failure scenario. This is regarded as failures caused by traffic concentration on the node in a single virtual network. Note that, in all scenarios, the failures occur at a node in the topology at lowest hierarchy. The random and hub node failures continue until the 15% of nodes in the topology is removed.

5.2.3 Results

First of all, Figure 15 reveals the effect of the difference of the construction method of inter-module links. The evaluated topologies are generated by parameter $m = 2$. Note that the topologies with fractality are MINSG and C[0.0]. In this figure, y-axis shows $T_{f_0}^1$, or reachability at the lowest topology. The figure shows MINSG and C[0.0] can hold high reachability under the failure of both terminal nodes of inter-module links and hub node. On the other hand, reachability of other topologies decreases faster than MINSG and C[0.0]. For the random node failure, all topologies show the similar changes of reachability before the failure ratio reaches around 0.1. After that, reachability of MIN, C[1.0] and C[0.0] decreases. Taking a practical situation into consideration, however, it is unlikely to occur the node failure more than 10% in a topology. Therefore, MINSG and C[0.0], that is, the fractal topologies have robustness against various types of the failures.

Next, Figure 16 shows the effect of the parameter m in our proposed method. The evaluated topologies are generated by C[0.0] with different m. Note that the parameters $m = 2, 4$ and 8 generate the fractal topologies, on the other hand, the parameter $m = 64$ generates the non-fractal topology. In this figure, y-axis shows reachability at the lowest topology. This figure shows the fractal topologies exhibit the robust behavior against various types of the failures regardless of parameter m. By contrast, the non-fractal topology shows the unrobust behavior due to the rapid decrease of reachability.

Finally, Figure 17 shows the transition of reachability of the topology at higher hierarchy, or module-level topology. The evaluated topologies are generated by C[0.0] with $m = 2$. This figure reveals that reachability of module-level topology is highly maintained even if reachability of the topology at the lowest hierarchy decreases (red line). This means the hierarchical modular structure contributes to suppression of impacts of loss of reachability.

Summarizing the above, the fractal topology is robust against various types of node failures. In addition, thanks to its hierarchical structure, the fractal topology is able to suppress impacts of loss of connectivity.

5.3 Node Betweenness Centrality

Node betweenness centrality $g(v)$ of node v is defined by following equation:

$$g(v) = \sum_{s,t \in V} \frac{\sigma_{st}(v)}{\sigma_{st}}, \qquad (7)$$

where, V is the set of nodes, σ_{st} is the number of shortest paths between node s and node t, and $\sigma_{st}(v)$ is the number of those paths passing through node v. Note that if $s = t$, $\sigma_{st} = 1$, and if $v \in \{s, t\}$, $\sigma_{st}(v) = 0$. The higher $g(v)$ means that there is more paths passing through node v, that is, node v may suffer from the high load.

First, figure 18 shows the result of topology with 8192 nodes. From this result, regardless of parameter m, MINSG and C[0.0] can keep $g(v)$ low compared to the others. The other methods for constructing inter-module links except MINSG and C[0.0] have links between hub nodes, therefore, the load is concentrated on these nodes. On the other hand, MINSG and C[0.0] do not have links between hub nodes, hence, the load is distributed to many peripheral nodes.

Next, figure 19 shows the case of larger topology. This result reveals, even if the topology is getting large, MINSG and C[0.0] can avoid load concentration.

Taken together Figure 18 and 19, fractal topology can avoid traffic concentration.

5.4 Average Hop Length and Diameter

Figure 20 shows the evaluation results of average hop length and diameter. First, compared with each method of constructing inter-module links, MINSG takes the largest value followed by C[0.0], C[1.0], C[2.0] and C[3.0]. This results from the difference of contribution of hub nodes for inter-module links. Next, compared with each parameter m, larger m takes smaller value in both average hop length and diameter. We use star topology as module-level topology. Hence, larger m means connecting a larger number of nodes with almost same hop length compared to smaller m. This is the reason larger m can communicate via shorter paths.

Figure 21 and 22 show the increasing ratio of average hop length and diameter respectively. The values in the figures are normalized by the value of $h = 7$. These figures reveal that, as topology is getting larger, the topology which tends to connect between non-hub nodes further increase its path length compared to the topology which tends to connect between hub nodes.
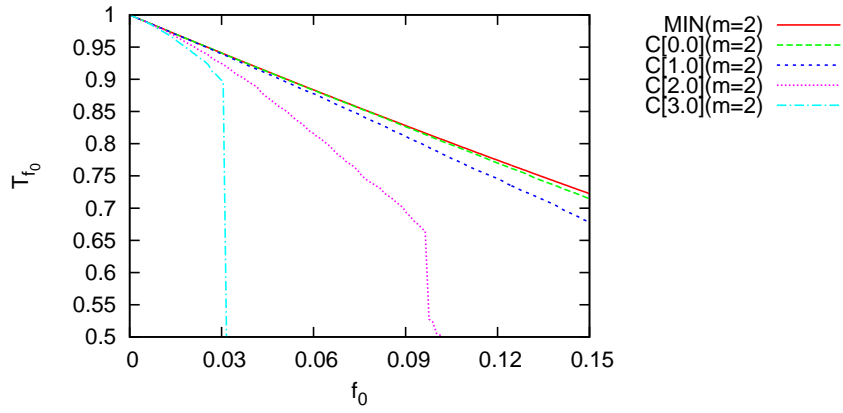
(a) Failure of both terminal nodes of inter-module links
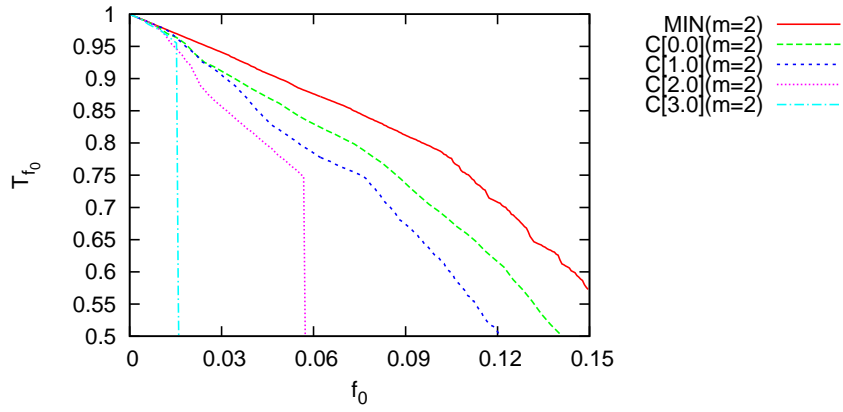
(b) Failure of hub node
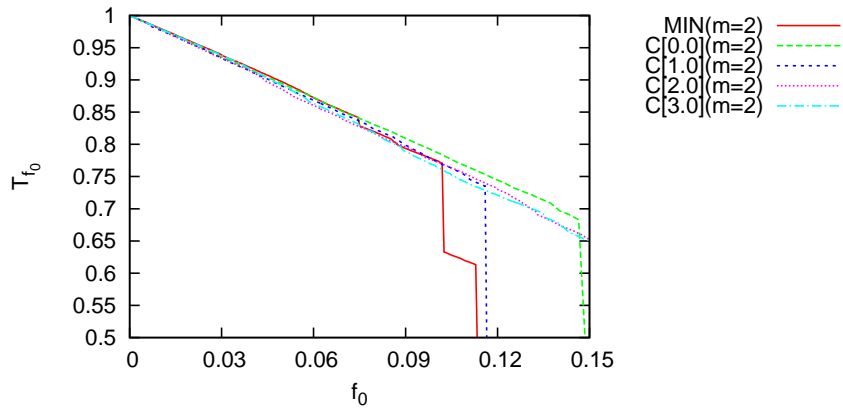
(c) Failure of randomly selected node

Figure 15: Reachability under node failures as a function of failure ratio f_0 : Difference of the construction method of inter-module links
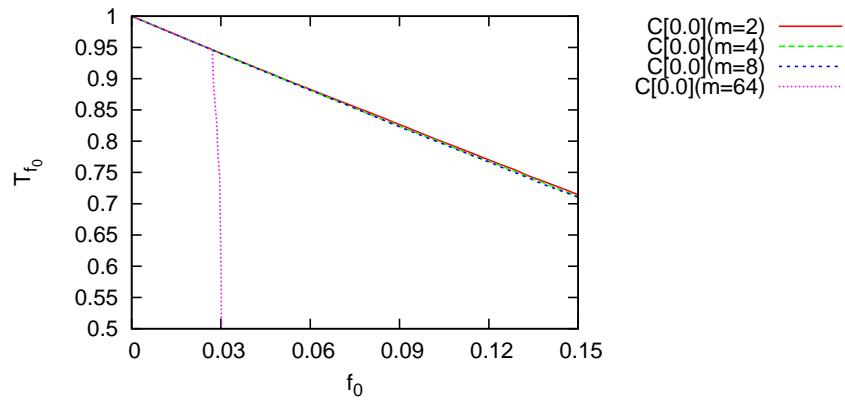
(a) Failure of both terminal nodes of inter-module links
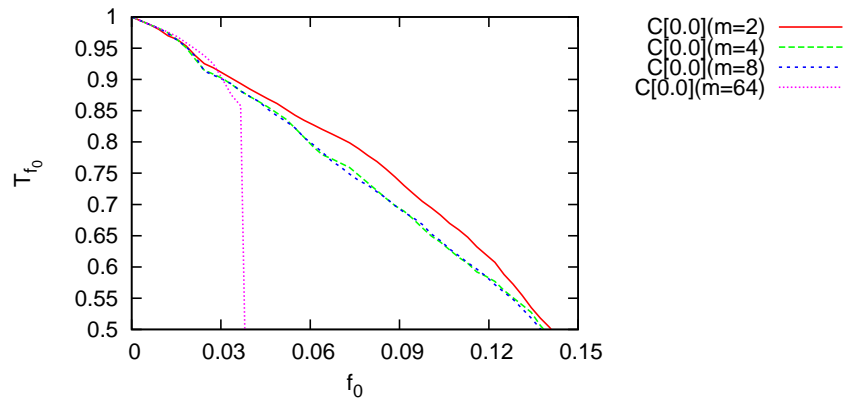
(b) Failure of hub node
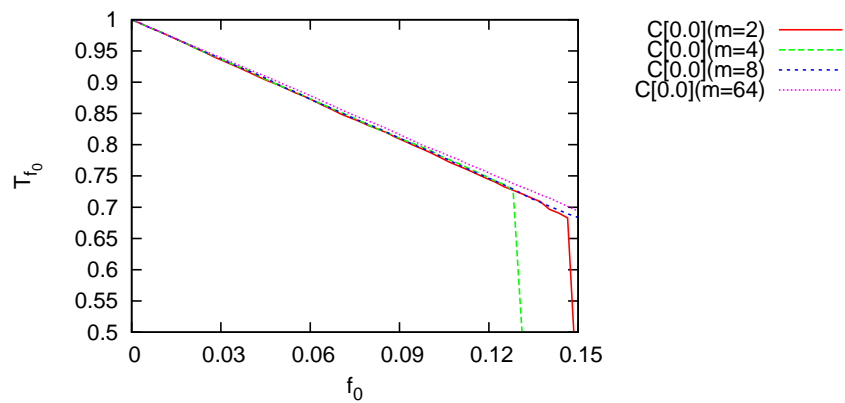
(c) Failure of randomly selected node

Figure 16: Reachability under node failures as a function of failure ratio f_0 : Difference of parameter m
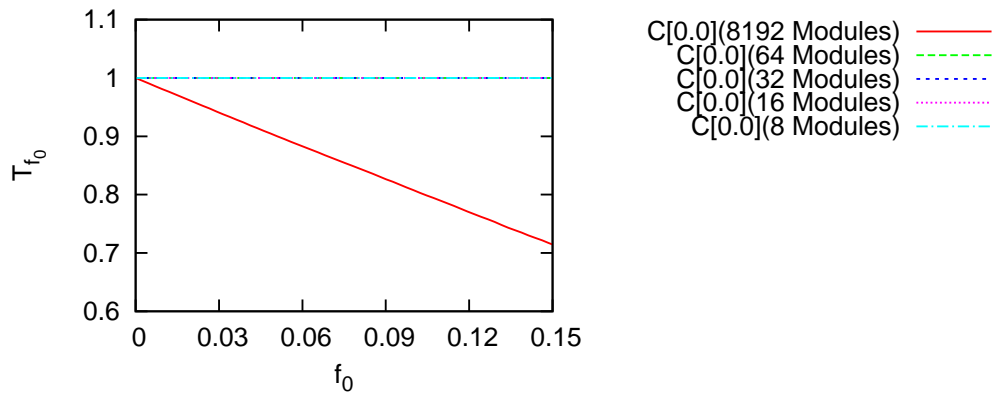
(a) Failure of both terminal nodes of inter-module links
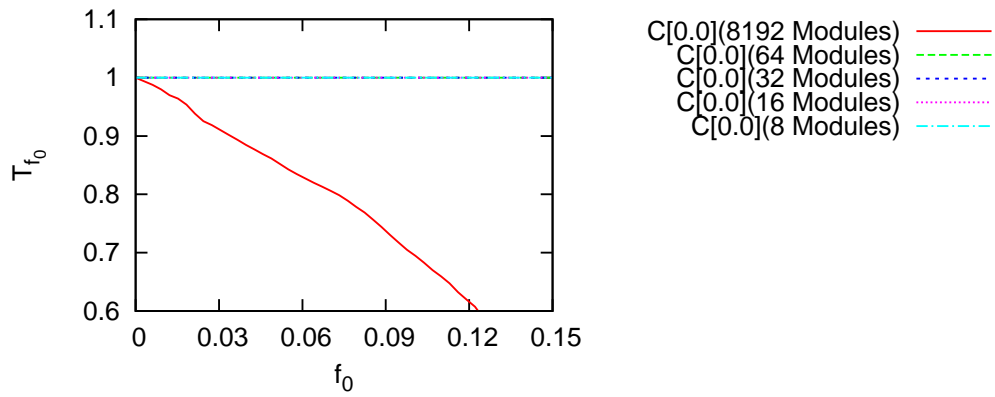
(b) Failure of hub node
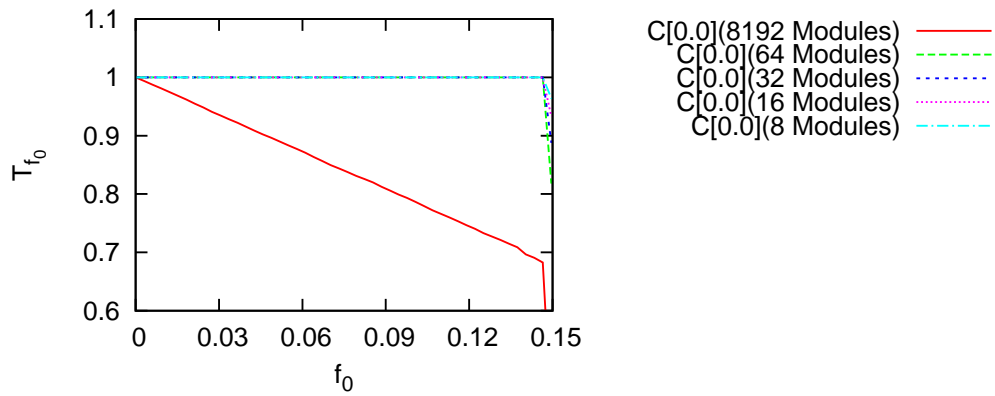
(c) Failure of randomly selected node

Figure 17: Reachability under node failures as a function of failure ratio f_0 : Topology at higher hierarchy
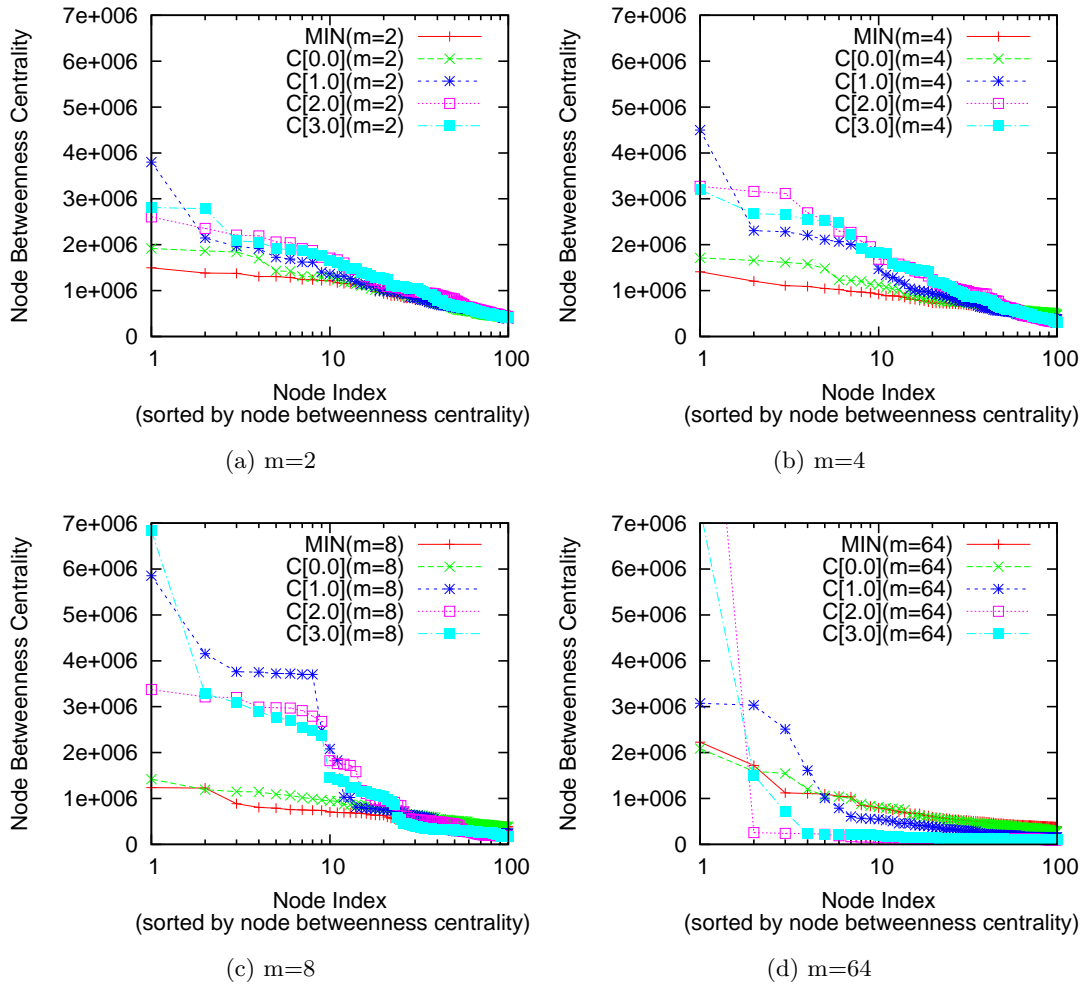
Figure 18: Node betweenness centrality : $N = 8192$
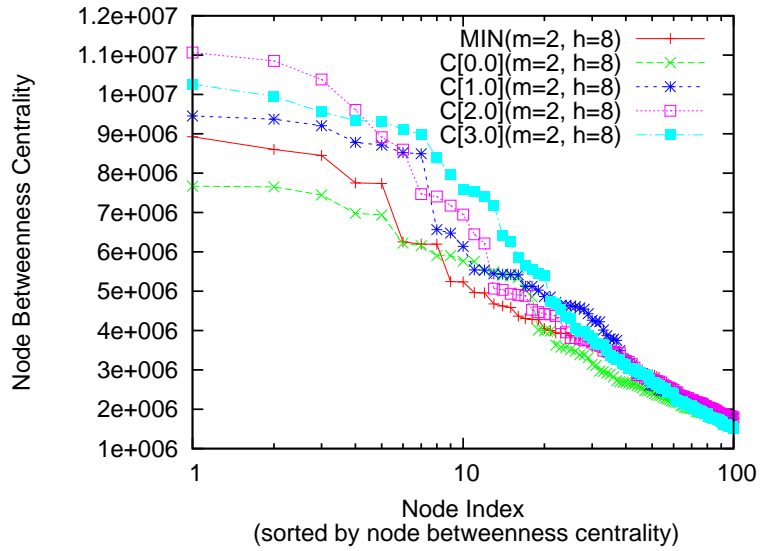
(a) h=8
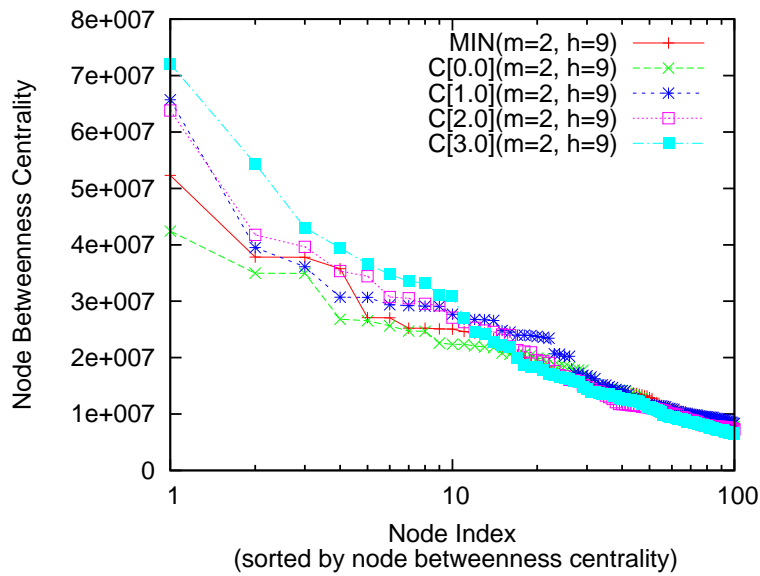
(b) h=9

Figure 19: Node betweenness centrality for larger topology : $N = 16384$ and 32768
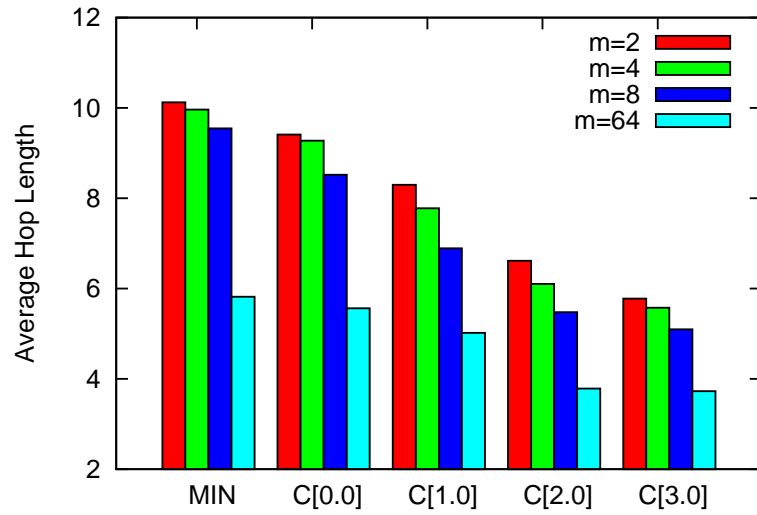
(a) Average hop length
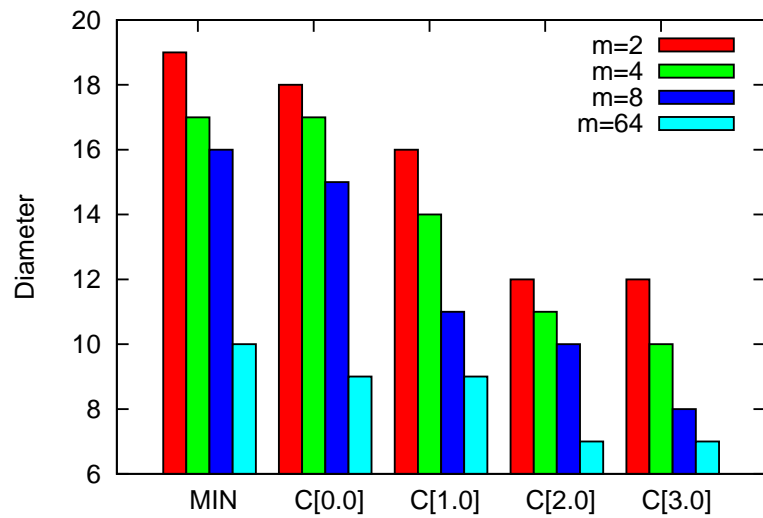
(b) Diameter

Figure 20: Average hop length and diameter : $N = 8192$
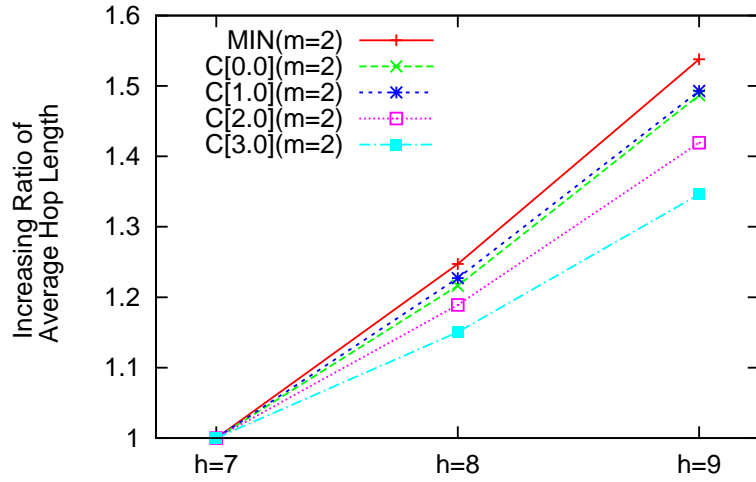
Figure 21: Increasing ratio of average hop length for larger topology : $N = 16384$ and 32768
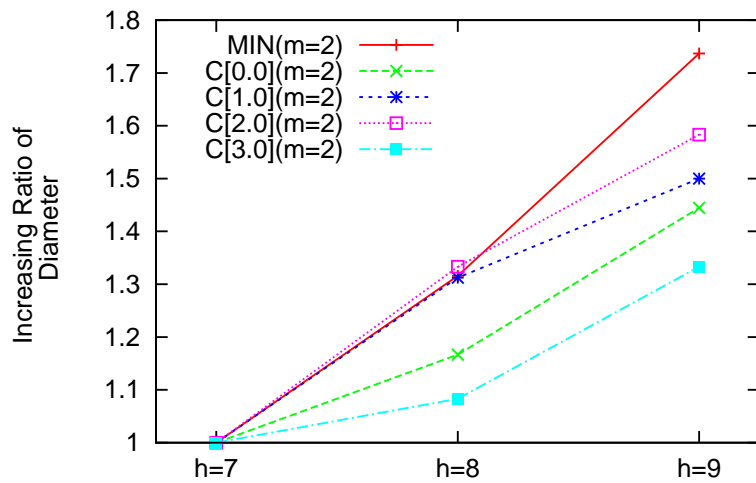
Figure 22: Increasing ratio of diameter for larger topology : $N = 16384$ and 32768

6   Conclusion

In this thesis, we proposed the configuration method of virtual networks with fractality to maintain the connectivity, suppress impacts of loss of connectivity into a small range, and relax the traffic or load concentration. Our method configures a hierarchical modular virtual network by piling up a single virtual network as a module. The key to fractality is the way to connecting modules. We revealed that we can generate the fractal topology by avoiding construction of inter-module links between hub nodes. Moreover, the topology without the hierarchical structure cannot possess fractality even if inter-module links are constructed between non-hub nodes. We evaluated the topological performance of the fractal and non-fractal topologies. The results showed the fractal topologies can keep reachability between modules against the various types of node failures and relax the traffic concentration. On the other hand, hop length tends to be longer due to the absence of hub-hub connection.

We used specific parameters for our evaluation in this thesis, however, out proposed method has many parameters to be considered. In addition, we have to consider the different module-level topology in our proposed method other than the star topology. Therefore, as the future work, we evaluate the fractality and performance by using various parameters.

Acknowledgements

References

[1] N. M. K. Chowdhury and R. Boutaba, "A survey of network virtualization," *Computer Networks*, vol. 54, pp. 862–876, Apr. 2010.

[2] A. Wang, M. Iyer, R. Dutta, G. N. Rouskas, and I. Baldine, "Network virtualization: Technologies, perspectives, and frontiers," *Journal of Lightwave Technology*, vol. 31, pp. 523 – 537, Feb. 2013.

[3] Ministry of Internal Affairs and Communications, "Accident situation of telecommunications services (FY2014) (in Japanese)." `http://www.soumu.go.jp/menu_seisaku/ictseisaku/net_anzen/jiko/result.html`, July 2015.

[4] E. Bullmore and O. Sporns, "Complex brain networks: graph theoretical analysis of structural and functional systems," *Nature Reviews Neuroscience*, vol. 10, pp. 186–198, Mar. 2009.

[5] O. Sporns and R. F. Betzel, "Modular brain networks," *Annual Review of Psychology*, vol. 67, pp. 613–640, Jan. 2016.

[6] E. Bullmore and O. Sporns, "The economy of brain network organization," *Nature Reviews Neuroscience*, vol. 13, pp. 336–349, Apr. 2012.

[7] F. Klimm, D. S. Bassett, J. M. Carlson, and P. J. Mucha, "Resolving structural variability in network models and the brain," *PLoS Computational Biology*, vol. 10, p. e1003491, Mar. 2014.

[8] S. Ishikura, "Assortativity's effect on efficiency and robustness in inter-connected networks," Master's thesis, Osaka University, Feb. 2016.

[9] D. Meunier, R. Lambiotte, and E. T. Bullmore, "Modular and hierarchically modular organization of brain networks," *Frontiers in Neuroscience*, vol. 4, pp. 1–11, Dec. 2010.

[10] L. K. Gallos, H. A. Makse, and M. Sigman, "A small world of weak ties provides optimal global integration of self-similar modules in functional brain networks," *Proceedings of the National Academy of Sciences*, vol. 109, pp. 2825–2830, Feb. 2012.

[11] C. Song, S. Havlin, and H. Makse, "Origins of fractality in the growth of complex networks," *Nature Physics*, vol. 2, pp. 275–281, Apr. 2006.

[12] Y. Shijo, S. Arakawa, and M. Murata, "Topological analysis of the brain functional networks," in *Proceedings of the 8th International Conference on Bio-inspired Information and Communications Technologies (formerly BIONETICS)*, pp. 352–358, Dec. 2014.

[13] C. Song, S. Havlin, and H. Makse, "Self-similarity of complex networks," *Nature*, vol. 433, pp. 392–395, Jan. 2005.

[14] L. K. Gallos, M. Sigman, and H. A. Makse, "The conundrum of functional brain networks: Small-world efficiency or fractal modularity," *frontiers in Physiology*, vol. 3, pp. 1–9, May 2012.

[15] L. K. Gallos, F. Q. Potiguar, J. S. A. Jr, and H. A. Makse, "Imdb network revisited: Unveiling fractal and modular properties from a typical small-world network," *PLOS ONE*, vol. 8, pp. 1–8, June 2013.

[16] K.-I. Goh, G. Salvi, B. Kahng, and D. Kim, "Skeleton and fractal scaling in complex networks," *Physical Review Letters*, vol. 96, pp. 1–4, Jan. 2006.

[17] H. D. Rozenfeld, S. Havlin, and D. ben Avraham, "Fractal and transfractal recursive scale-free nets," *New Journal of Physics*, vol. 9, pp. 1–16, June 2007.

[18] B. Guo, C. Qiao, J. Wang, H. Yu, Y. Zuo, J. Li, Z. Chen, , and Y. He, "Survivable virtual network design and embedding to survive a facility node failure," *Journal of Lightwave Technology*, vol. 32, pp. 483–493, Feb. 2014.

[19] "SPM - Statistical Parametric Mapping." [online] `http://www.fil.ion.ucl.ac.uk/spm/`.

[20] V. Blondel, J. Guillaume, R. Lambiotte, and E. Mech, "Fast unfolding of communities in large networks," *Journal of Statistical Mechanics*, pp. 1–12, July 2008.

[21] J. Y. Yen, "Finding the k shortest loopless paths in a network," *Management Science*, vol. 17, pp. 712–716, July 1971.

[22] A.-L. Barabási and R. Albert, "Emergence of scaling in random networks," *Science*, vol. 286, pp. 509–512, Oct. 1999.

[23] D. Watts and S. Strogatz, "Collective dynamics of 'small-world' networks," *Nature*, vol. 393, pp. 440–442, June 1998.

[24] M. P. van den Heuvel, C. J. Stam, R. S. Kahn, and H. E. Hulshoff Pol, "Efficiency of functional brain networks and intellectual performance," *The Journal of Neuroscience*, vol. 29, pp. 7619–7624, June 2009.

[25] B. M. Waxman, "Routing of multipoint connections," *IEEE Journal on Selected Areas in Communications*, vol. 6, pp. 1617–1622, Dec. 1988.

[26] A. F. Alexander-Bloch, P. E. Vértes, R. Stidd, F. Lalonde, L. Clasen, J. Rapoport, J. Giedd, E. T. Bullmore, and N. Gogtay, "The anatomical distance of functional connections predicts brain network topology in health and schizophrenia," *Cerebral Cortex*, vol. 23, pp. 127–138, Jan. 2012.

[27] R. Albert, H. Jeong, and A. Barabàsi, "Error and attack tolerance of complex networks," *Nature*, vol. 406, pp. 378–382s, July 2000.

[28] R. K. Pan and S. Sinha, "Modular networks with hierarchical organization: The dynamical implications of complex structure," *Indian Academy of Sciences*, vol. 71, pp. 331–340, Aug. 2008.

[29] L. Li, D. Alderson, R. Tanaka, J. C. Doyle, and W. Willinger, "Towards a theory of scale-free graphs: definition, properties," tech. rep., California Institute of Technology, Pasadena, CA, USA, Oct. 2005.